Dynamic vortex instabilities in Ta/Ge-based multilayers and thin films with various pinning strengths

B. J. Ruck* and H. J. Trodahl
School of Chemical and Physical Sciences, Victoria University of Wellington, P.O. Box 600, Wellington, New Zealand

J. C. Abele
Department of Physics, Lewis and Clark College, Portland, Oregon 97219

M. J. Geselbracht
Department of Chemistry, Reed College, Portland, Oregon 97202

(Received 30 May 2000)

We report measurements of a dynamic instability in the moving vortex system of Ta/Ge-based thin films and multilayers. The instability results from a nonequilibrium distribution of quasiparticles induced by motion of the vortex cores, as described theoretically by Larkin and Ovchinnikov in the regime where there is no pinning. For the Ta/Ge system, where the critical vortex velocity is relatively small, we observe the instability in cases where either the viscosity or pinning dominate the vortex motion. We develop a simple model to describe the effects of pinning on the flux motion near the instability, and show that it gives a good description of the experimental data, especially in fields not too close to zero. The temperature dependence of the critical vortex velocity extracted from the analysis indicates that electron-electron scattering provides the dominant contribution to the energy relaxation.

I. INTRODUCTION

It is well known that an applied current can induce motion of magnetic flux lines in type-II superconductors, leading to the appearance of a finite resistance. This phenomenon has been studied intensively in the low current limit where, in the presence of pinning, the type of flux motion depends sensitively on whether the vortices are in a liquid or a glassy state.[1] The corresponding high current limit is also of considerable interest, both from a theoretical and applied perspective. In general it is expected that as the current is increased the relevance of pinning decreases, and the resistance will tend towards a constant free flux flow limit. However, in this regime Larkin and Ovchinnikov (LO) have predicted a fundamental instability in the freely moving vortex system, which results in a transition from the flux flow state back into the normal state.[2,3] This instability can occur well before the depairing critical current is reached, and thus sets an upper limit on the current at which superconducting order can be maintained.

LO instabilities have been observed in both high-T_c (Refs. 4–11) and low-T_c (Refs. 12–14) systems, including Ta/Ge based multilayers and alloys.[15] In this paper we extend our work on the Ta/Ge system to examine LO instabilities in multilayers with varying degrees of anisotropy. Due to the different dimensionalities, the multilayers exhibit different vortex phases in the current regime immediately before the instability takes place, with a corresponding variation in the pinning strengths. We demonstrate that, although the pinning has a strong effect on the vortex dynamics, the instability is still present and has the same fundamental nature, i.e., it results from the existence of a maximum in the total retarding force on the vortices as a function of vortex velocity. We propose a simple model to incorporate the effects of pinning into the vortex dynamics close to the instability, and show that it provides good agreement with the experimental data.

II. DYNAMIC VORTEX INSTABILITIES

A. Larkin-Ovchinnikov instabilities

Larkin and Ovchinnikov calculated the correction to the distribution function caused by the electric field produced when an applied current forces the vortices to move. They found that the electric field shifts the nonequilibrium distribution of quasiparticles in the vortex core to higher energies, causing some of the quasiparticles to diffuse into the surrounding area. This in turn causes the vortex core to shrink according to the formula

$$\xi^2(v) = \frac{\xi^2(0)}{1+(v/v^*)^2}, \tag{1}$$

where v is the vortex velocity, $\xi(0)$ is the Ginzburg-Landau coherence length at $v=0$, and v^* is a characteristic critical vortex velocity. The decrease of ξ in the vicinity of the vortices leads to a reduction in the viscous damping coefficient η given by $\eta(v)=\eta(0)/[1+(v/v^*)^2]$, and the viscous force $\eta(v)v$ has a maximum at the critical velocity v^*. Any increase in velocity past v^* causes a reduction in the damping force which further perpetuates the velocity increase, and thus the vortex system becomes unstable. The critical velocity is determined by the formula

$$v^{*2} = \frac{D[14\zeta(3)]^{1/2}(1-T/T_c)^{1/2}}{\pi\tau_{\text{in}}}, \tag{2}$$

where $D=(v_f l)/3$ is the quasiparticle diffusion coefficient with v_f the Fermi velocity and l the electron mean free path,

τ_{in} is the inelastic-scattering time of the quasiparticles, and $\zeta(3)=1.202$ is the Riemann ζ function of 3. For longer values of τ_{in}, the nonequilibrium quasiparticles relax more slowly, resulting in a greater deviation from equilibrium in the distribution function. The nonlinear effects of the LO theory are thus most noticeable in materials with large values of τ_{in} or small values of D, both of which are characteristic of amorphous Ta or Ta_xGe_{1-x} at low temperature.

The voltage at which the instability occurs is related to the critical vortex velocity by

$$V^*=\mu_0 v^* HL, \tag{3}$$

where L is the length between the voltage probes. Close to the instability the current-voltage (I-V) curve begins to show the effects of the change in the viscosity. Samoilov *et al.*[14] give the following form for the I-V characteristic:

$$I=\frac{V}{R_n}\left[\frac{\alpha}{1+(V/V^*)^2}+1\right], \tag{4}$$

in which R_n is the normal state resistance. The first term in the brackets represents the effects of the decrease in vortex core radius, while the second term accounts for suppression of superconductivity outside the vortex cores by the electric field. For $\alpha>8$ Eq. (4) predicts a back-bending I-V curve which shows negative differential resistance beginning in the vicinity of V^*. In the current biased mode the negative differential resistance is manifested as a sharp jump in the I-V curves to a resistance close to the limiting value R_n. The backbending curve allows for the possibility that the critical current I^* where the transition occurs is lower on a downward sweep than on an upward sweep, resulting in a hysteresis. For $\alpha\leqslant 8$ the back-bending is no longer evident, and instead a rapid but continuous rise in the I-V characteristic is expected. Equation (4) has been used successfully to describe the I-V characteristics of an a-Mo_3Si thin film[14] for a range of field values.

In the LO theory the instability is predicted in the regime of temperatures close to T_c, where the conductivity is most sensitive to changes in the distribution function. The parameter α in Eq. (4) is related to the flux flow conductivity σ in the limit of low vortex velocity. The result for σ in the temperature range near T_c, and in fields not too close to H_{c2}, leads to an expression for α given by

$$\alpha=\frac{\mu_0 H_{c2}(T)}{B(1-T/T_c)^{1/2}}\tilde{f}(B/\mu_0 H_{c2}), \tag{5}$$

where the function $\tilde{f}(B/\mu_0 H_{c2})$ is equal to 4.04 at low fields, and decreases with field thereafter.[3] At low fields α is large and the nonlinear effects described by Eq. (4) are significant, whereas at high fields α is small and the non-linear effects are weak.

Equation (2) predicts that v^* decreases with temperature as $(1-T/T_c)^{1/4}$, as observed in early experiments.[12,13] More recently Doettinger *et al.*[4,7] and Xiao *et al.*[11] have measured a critical vortex velocity which instead increases with temperature. This was well described by including either an $\exp[2\Delta(T)/k_BT]$ or an $\exp[4\Delta(T)/k_BT]$ form for the temperature dependence of τ_{in} [$\Delta(T)$ is the superconducting energy gap].

B. Modifications to the LO theory

The basic LO theory outlined above includes several assumptions. Firstly, it is assumed that heat is removed effectively from the lattice which remains in thermal equilibrium with the bath. Recently Bezuglyj and Shklovskij[16] (BS) have extended the LO theory to the case where there is a finite heat removal rate from the sample to the substrate, such that some heating of the sample is unavoidable. The linear heat balance equation

$$h(T_q-T_b)=IV/wL \tag{6}$$

is solved simultaneously with Eq. (4) to find the instability point $(I^*_{T_q}, V^*_{T_q})$ (h is the total heat transfer coefficient from the quasiparticles to the bath, T_q is the effective quasiparticle temperature, T_b is the bath temperature, and w is the width of the sample). Two regimes of magnetic field are found, separated by a characteristic field $B_T=0.37e\tau_{in}h/k_B\sigma_n d$ (σ_n is the normal state conductivity, and d is the sample thickness). When $B\ll B_T$ heat is removed effectively from the sample and v^* is given by Eq. (2). For $B\gg B_T$ sample heating is important and the measured value of v^* decreases well below its value in low fields. In this case the heating effect dominates the distribution function, and the instability results mainly from the decrease in conductivity caused by heating rather than from the field induced nonequilibrium quasiparticle distribution. Excellent agreement with this theory has been found by Xiao *et al.*[9,11] in a range of high-T_c superconducting films.

Secondly, it is assumed that the non-equilibrium quasiparticle distribution is homogeneous throughout the sample. This will be the case as long as the diffusion length $(D\tau_{in})^{1/2}$ exceeds the intervortex spacing a_0, allowing the quasiparticles to diffuse fully into the superconductor before they relax. A similar requirement has been shown[5] to lead to an increase in the measured value of v^* proportional to $a_0=1.07(\Phi_0/B)^{1/2}$ at low fields ($\Phi_0=2.07\times10^{-15}\,\mathrm{Tm}^2$ is the magnetic flux quantum).

Finally, it is assumed that pinning plays no role in determining the I-V characteristics. Some experiments are deliberately designed to be in this regime,[6,7,9,11,14] in which case the LO theory, including the above modifications, describes the data well. In other cases a lack of linearity in the I-V characteristic below the instability point indicates that pinning can be a significant factor in determining the vortex motion.[8,15] We explore the consequences of this in the following sections.

III. EXPERIMENTAL METHOD

A selection of amorphous Ta/Ge and Ta_xGe_{1-x}/Ge ($x\approx 0.3$–0.4) multilayers and thin films were grown by evaporative deposition of the Ta and Ge onto glass substrates in an ultra high vacuum chamber with a base pressure of less than 10^{-9} torr. The multilayers thus produced were characterized by x-ray fluorescence or Rutherford backscattering spectroscopy, multiple beam interferometry, x-ray

TABLE I. Parameters defining the morphology and superconducting characteristics of each of the samples. d_s is the superconducting layer thickness, d_i is the insulating Ge layer thickness, %Ta gives the percentage of Ta in the superconducting layers, and $S_\parallel$ is equal to $-\mu_0 dH_{c2}/dT|_{T=T_c}$.

Sample	Layers	d_s (Å)	d_i (Å)	%Ta	T_c (K)	$S_\parallel$ (T/K)	$\xi_\parallel(0)$ (Å)	$\lambda_\parallel(0)$ (Å)	γ
A	12	60±10	170±9	38±3	2.28	2.2±0.1	81±2	11000±2000	∞
B	12	60±10	170±9	38±3	2.27	2.1±0.3	83±6	11000±2000	∞
C	8	210±40	180±10	45±3	2.66	1.8±0.1	83±2	11000±2000	∞
D	13	40±10	30±5	25±2	1.85	1.9±0.1	96±3	14000±2000	5.8
E	25	25±2	24±2	100	1.66	1.9±0.1	102±3	12000±2000	1.5
F	1	670±70	0	27±2	2.80	2.1±0.3	75±5	11000±2000	

diffraction (XRD), and transmission electron microscopy to determine the layer thicknesses and alloy layer composition.[17,18] The films were confirmed amorphous by the XRD measurements, and also by the absence of any sign of a superconducting transition at 4.2 K, the T_c of crystalline Ta. The morphologies of the samples used in this investigation are summarized in Table I. Each of the samples was patterned into a bridge of width approximately 1 mm and length approximately 5 mm for four terminal resistance measurements. The samples were placed directly in the liquid helium bath to minimize any heating effects. Almost all of the data presented below were taken at temperatures below the lambda point (2.17 K) where the stability was better than ± 1 mK. In all cases the field was oriented perpendicular to the plane of the layers.

The superconducting transition temperature and the upper critical fields of each sample were determined by fitting to the fluctuation conductivity above the transition.[19,20] Perpendicular field data allowed a determination of the in-plane coherence length $\xi_\parallel$ and the penetration depth for in-plane currents $\lambda_\parallel$, while corresponding parallel field data yielded the anisotropy of the samples $\gamma=\xi_\parallel/\xi_\perp$ ($\xi_\perp$ is the coherence length perpendicular to the layers).[21] The results of this analysis are presented in Table I, where it can be seen that all of the samples are strongly type II, with $\kappa=\lambda_\parallel(0)/1.63\xi_\parallel(0)$ varying between 70 and 90. For samples A, B, and C the parallel critical field showed a square root temperature dependence characteristic of two-dimensional behavior, corresponding to fully decoupled layers. Due to the amorphous nature of the films the resistivity is very high, being around 200 $\mu\Omega$ cm. Values determined previously[17,18] for the Fermi velocity $v_f \approx 2.4\times10^6$ m/s and the electron mean free path $l \approx 1.5$ Å can be used to calculate the diffusion coefficient $D=(v_f l)/3 \approx 1\times10^{-4}\,\mathrm{m^2/s}$. Alternatively, the diffusion coefficient can be estimated[21] from $D=(4k_B/\pi e)(-dH_{c2}/dT|_{T=T_c})^{-1}$ yielding a similar value $D\approx 5\times10^{-5}\,\mathrm{m^2/s}$, which we use below.

IV. RESULTS AND ANALYSIS

In a previous study[15] we reported observations of a current induced instability in the I-V characteristics of two of the above samples (E and F), which was manifested as a sharp jump in the I-V curves at low magnetic fields, crossing over to a broader transition at high fields. The same instability was observed on both downward and upward current sweeps, despite several orders of magnitude difference in the input power at the transition in the two cases. Furthermore, a quantitative agreement was found between the measured critical vortex velocities and the LO prediction, where the predicted value was calculated from Eq. (2) using parameters determined independently from the normal state properties. This showed conclusively that the instability was of the LO type. We have since performed similar measurements on the rest of the samples described above, which we will now discuss in turn beginning with the samples which showed the least effects of vortex pinning, before moving to samples for which pinning effects are clearly important.

A. Low vortex pinning regime

Figure 1(a) shows a set of I-V curves taken from sample A at a temperature of 1.710 K, where each curve corresponds to a different magnetic field. Two qualitatively different field regimes can be identified. At low fields the curves display a nonlinear increase at low to intermediate current levels, before approaching linear behavior as high current levels are reached. For these curves the high current region is terminated by a sudden jump to a resistance close to the normal state value, indicating an instability in the flowing vortex system. At the four highest fields, on the other hand, the curves are linear at all but the highest currents, where a rapid but continuous rise toward the normal state resistance takes place. A thermally activated resistivity, characteristic of vortex pinning, can be measured only at low fields and currents, indicating that pinning effects are negligible near the instability.

Figure 1(b) shows a close up of a selection of the data near to the instability, where the solid lines show fits using Eq. (4). Only the data indicated by solid symbols has been used in the fitting. Figure 1(c) shows the fitted values of α as a function of field, where data from the similar sample B taken at 1.245 and 1.550 K are also included. At low fields the data show a H^{-1} field dependence, while at high fields a more rapid decrease in α is observed. This is in excellent agreement with Eq. (5) which for low fields predicts $\alpha \propto H^{-1}$, followed by a stronger dependence at high fields caused by the decrease in $\tilde{f}(B/\mu_0 H_{c2})$. Less accurate fitting was achieved for sample B at the lower temperatures because pinning dominated the I-V curves over a much larger range. Nevertheless α clearly decreases with temperature, reflecting the temperature dependence of H_{c2} in Eq. (5).

Evidently the LO theory captures very well the behavior of the I-V curves for samples with thin, decoupled superconducting layers, at least at temperatures close to T_c. This is

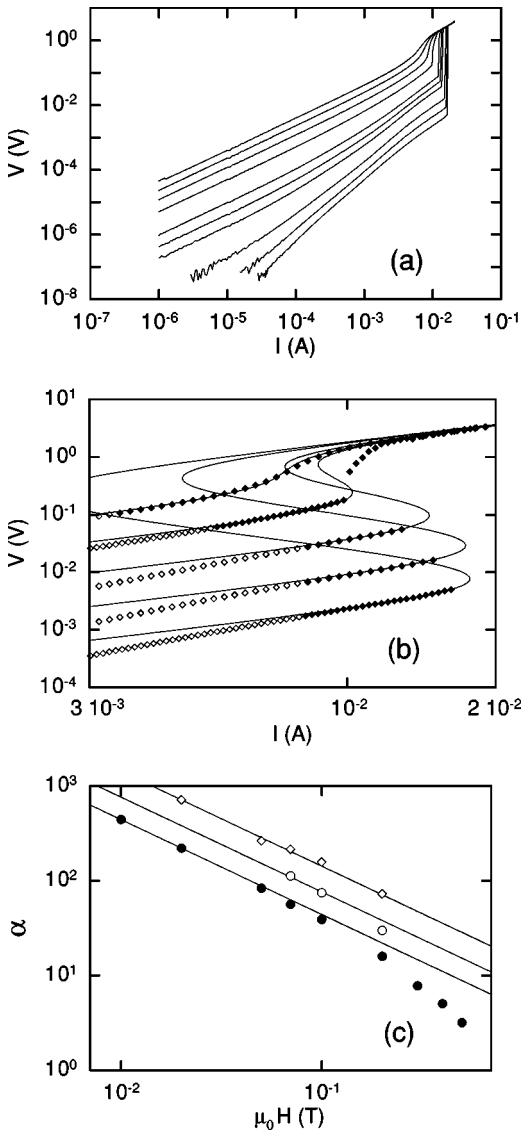

FIG. 1. (a) *I-V* curves from sample A measured at 1.71 K in fields (from right to left) of 0.005, 0.01, 0.02, 0.05, 0.07, 0.1, 0.2, 0.3, 0.4, and 0.5 T. (b) Enlarged view of the 0.005, 0.02, 0.07, 0.2, and 0.4 T curves. The solid lines are fits of Eq. (4) to the data, where only the solid points have been used in the fitting. (c) Fitted values of α for sample A at 1.71 K (●) and B at 1.55 K (○) and 1.245 K (◇). The solid lines show the field dependence $\alpha \propto H^{-1}$.

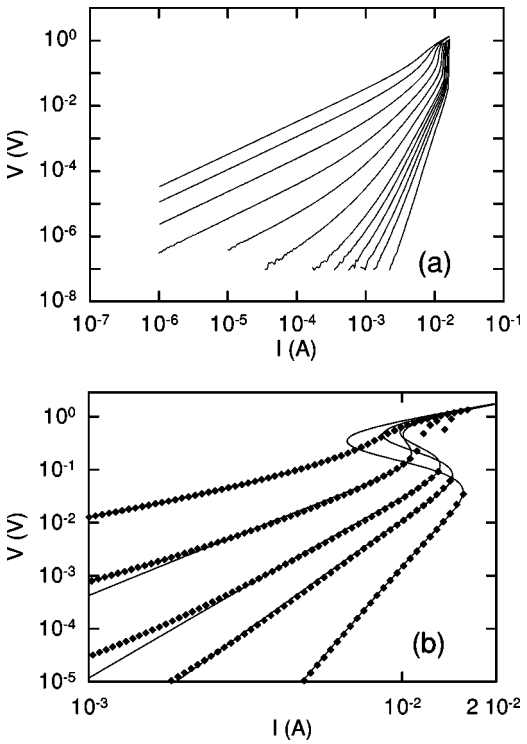

FIG. 2. (a) *I-V* curves from sample C in a field of 0.7 T. From right to left the curves correspond to temperatures of 1.21, 1.3, 1.35, 1.4, 1.45, 1.5, 1.6, 1.7, 1.8, 1.9, 2.0, and 2.1 K. (b) Enlarged view of the 1.21, 1.45, 1.6, 1.8 and 2.0 K curves. The solid lines are fits using Eq. (8).

expected because the low level of pinning makes it possible to observe a rather large free flux flow regime. It is interesting to note, however, that no hysteresis is observed in the current sweeps in Fig. 1, but instead the upward and downward sweeps are identical. Furthermore, the fitted value of v^* generally corresponds to a point slightly above the instability, indicating the vortex system may become unstable a little before the peak in the viscosity is reached. We will return to the discussion of v^* for all of the samples below.

B. Effects of vortex pinning

The current density where dissipation can first be observed is typically much higher in the other samples than it is for samples A and B, implying that pinning plays a more substantial role in the vortex dynamics. To demonstrate this we show in Fig. 2(a) a set of *I-V* curves taken from sample C at various temperatures, in a fixed field of 0.7 T. Instabilities very similar to those described above are observed, including development from sharp to broad transitions as the temperature is increased. The similarity between the instability in this sample and in A and B implies that the underlying mechanism is the same in each case. However, in Fig. 2(a) the degree of non-linearity is far greater than in Fig. 1. In fact, for the entire range of temperatures, there is no region of linear *I-V* behavior near the instability corresponding to free flux flow.

Although attempts have been made to fit the curves of Fig. 2(a) to Eq. (4) in the same manner shown in Fig. 1, no reasonable results could be obtained, implying that pinning must be taken into account in order to describe these data. To do this we follow the dynamic approach of Blatter *et al.*[1] in which the relative correction $\delta v/v$ to the vortex velocity caused by pinning is calculated. In the dynamic approach pinning can be considered as a friction term which, by symmetry, must be directed opposite to the vortex motion. The coefficient of pinning friction η_p can be expressed in terms of the usual vortex viscosity coefficient η through the correction $\delta v/v$, leading to a pinning force

$$F_p = \eta_p v = (\eta \delta v/v) v. \tag{7}$$

As the vortex velocity in the present samples can approach v^* even when pinning dominates, account must also be taken of the decrease in the vortex core size described in the LO theory [Eq. (1)]. To do this we make the assumption that the pinning force varies linearly with the area of the

core.[22] We therefore use $\eta = \eta(0)/[1+(v/v^*)^2]$ in Eq. (7), which satisfies the requirement that the pinning should dramatically decrease above the instability, as the experimental data clearly show. The above arguments imply that the addition of pinning forces simply renormalizes the vortex viscosity in the LO theory. Therefore, Eq. (4) should be modified to

$$I = \frac{V}{R_n}\left[\frac{\alpha(1+\delta V/V)}{1+(V/V^*)^2}+1\right], \tag{8}$$

in which we have made the substitution $\delta v/v = \delta V/V$. It thus remains to determine the form of $\delta v/v$, which will in general depend on the field and temperature. Blatter *et al.* consider pinning as a perturbation, and derive different results for the correction depending on whether the vortices are in a liquid or solid-glass state. Larkin and Ovchinnikov have also studied a similar problem for both weak and strong pinning.[3]

The combined results for $\delta v/v$ indicate the existence of several different vortex velocity regimes characterized by different forms for the pinning correction, making it hard to fit a single function to the experimental I-V data. In all cases, however, $\delta v/v$ is a decreasing function of the vortex velocity, typically going as some negative power of v. To simplify matters we choose a general power law form $\delta V/V = \beta V^{-c}$, with a velocity independent value for the exponent c which can be extracted from the experimental data at low currents. Figure 2(b) shows a selection of the data from sample C close to the instability, where the solid lines are fits of Eq. (8) using α, β, and V^* as fitting parameters. Clearly this equation provides an extremely good description of the data, except at very low dissipation levels where thermally activated vortex motion dominates the resistivity and causes a linear region at low currents. Because the field is relatively high the contribution to the conductivity from the viscous force is small, which leads to very low values for α. As expected α is a decreasing function of the temperature. However at this field the uncertainty is too large to determine accurately the form of its temperature dependence.

C. Intermediate vortex pinning regime

Figure 3(a) shows a set of I-V curves taken from sample D at various temperatures in a fixed field of 0.3 T. The low temperature curves are highly nonlinear at low currents indicating that pinning forces are once again dominating the vortex motion. Unlike sample C, however, there is evidence of a crossover towards linear flux flow behavior at currents close to the instability. The solid lines are fits using Eq. (8) which once again provides an excellent description of the data, including the evolution from sharp to broad transitions at the instability. The values of α extracted from the fits show the same field dependence as samples A and B, consistent with the LO theory. Figure 3(b) shows the I-V data on a linear scale, where it can clearly be seen that the exact value of the resistance just above the transition depends on the field, but is always slightly less than the normal state value. This trend, which is also observed in the other samples, cannot be satisfactorily explained by any kind of heating effect; however, it can be modeled using Eqs. (4) and (8).

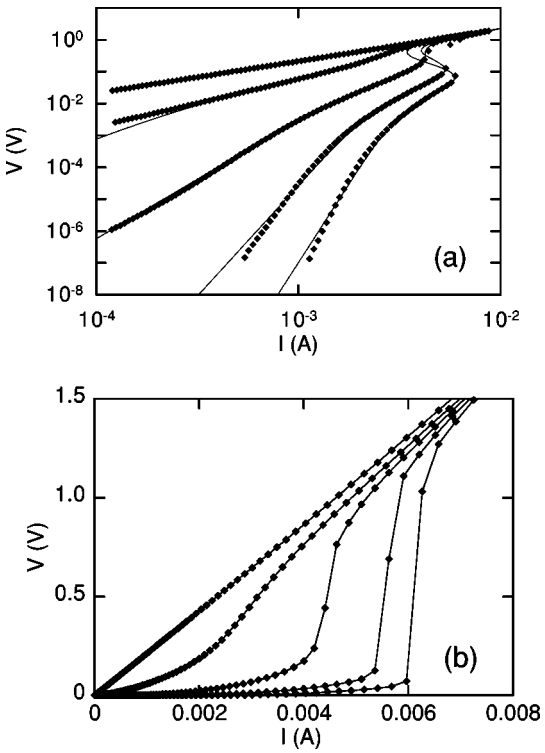

FIG. 3. (a) I-V curves from sample D in a field of 0.3 T. From right to left the curves correspond to temperatures of 1.22, 1.35, 1.5, 1.65, and 2.02 K. The solid lines are fits using Eq. (8). (b) The same data on a linear scale. Just above the instability the resistance is slightly less than the normal state value.

Figure 4(a) shows a set of I-V curves from sample E in various fields at 1.373 K. Similar to sample D, the I-V characteristics exhibit a transition from pinning dominated nonlinear behavior towards linear flux flow resistivity as the instability is approached. However, the range of fields where the instability can be clearly observed is considerably below the 0.3 T shown in Fig. 3. Our previous results on this sample demonstrated that the low current data could be well described within the vortex glass model[15] which also predicts a power law I-V characteristic,[23] lending further support to our choice for $\delta V/V$. Equation (8) is again successful in describing the data, although at the lowest fields it cannot capture the abruptness of the change in the resistivity, causing the fitted curves to bend backwards at current levels somewhat higher than the observed transition. Figure 4(b) shows a plot of the fitted values of α as a function of field for three different temperatures, where the variation is almost identical to the results for samples A and B for which no pinning term was considered. We note that the fitted values of β are approximately constant as a function of field or temperature for each of the samples C, D, and E, being in the range 2.1–2.6, 0.7–2, and 0.8–1.4, respectively. The exponent c is similar for all samples, varying between 0.5 and 0.9, with the larger values corresponding to lower fields and temperatures.

D. Critical vortex velocity

We now turn to a discussion of the values of the critical vortex velocity extracted from the above analysis. Firstly, we

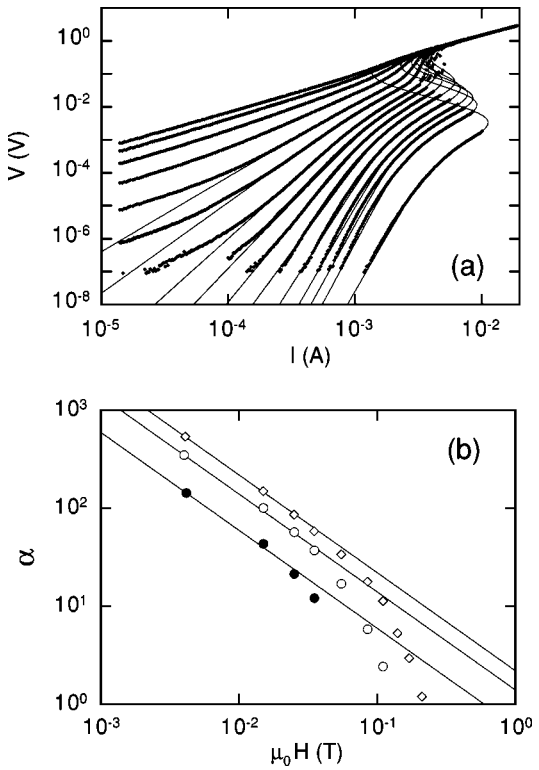

FIG. 4. (a) I-V curves from sample E at 1.373 K. From right to left the curves correspond to fields of 0.003, 0.015, 0.025, 0.035, 0.055, 0.085, 0.11, 0.14, 0.17, 0.21, 0.25, 0.3, 0.35, 0.4, and 0.45 T. (b) Fitted values of α for sample E at 1.520 K (●), 1.456 K (○), and 1.373 K (◇). The field dependence is the same as for samples A and B.

note that the values of V^* obtained from the fitting are slightly larger than the directly measured ones. This is already implicit in the original LO I-V equation in which the backbending occurs just above V^*, and is enhanced by our inclusion of a pinning term. Typically the difference is only slight, except at low fields where the instability transition is unusually sharp causing the fitted curve to extend beyond the data. Despite the difference in overall magnitude, the field and temperature dependence are approximately the same for both methods of determining v^*. Thus, the following conclusions are essentially independent of which method we choose to define V^*.

Figure 5 shows a plot of the fitted critical vortex velocity as a function of reduced magnetic field (H/H_{c2}) for sample A at 1.710 K, sample D at 1.220 K, and sample E at 1.373 K. Also shown is the critical velocity for sample D at 1.220 K determined directly from the measured voltage at the instability point. Except at the lowest fields, the fitted and directly measured values are in fairly close agreement, confirming the above statements regarding the two methods of determining v^*. Figure 5 also shows that v^* decreases with increasing applied field, with the dependence generally strongest at low fields. As discussed in Sec. II B there are several possible explanations for this behavior. Although we have already ruled out simple Joule heating as a significant effect, heating of the quasiparticles as in the BS theory can give a similar field dependence to that observed. The relevance of the BS theory to our data can be estimated by calculating the crossover field B_T above which quasiparticle heating effects

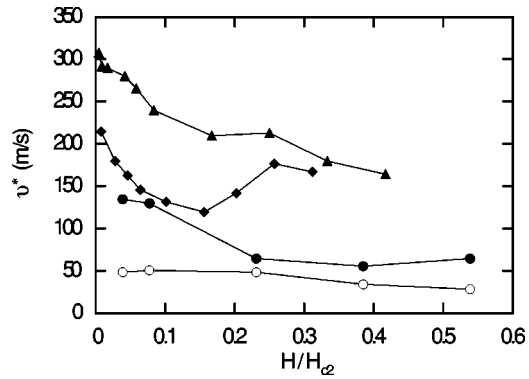

FIG. 5. Field dependence of the fitted critical vortex velocity for sample A at 1.710 K (▲), sample D at 1.220 K (●), and sample E at 1.373 K (◆). Also shown is v^* for sample D at 1.220 K (○) determined directly from the measured instability point.

become important. For the value of the heat transfer coefficient we take $h=10^4$ W/m^2 K. This is a conservative estimate based on measured values from a wide range of similar systems, and we note that for systems in contact with liquid helium below the superfluid transition the heat transfer coefficient is typically higher than our estimate.[24] An approximate value for τ_{in} may be determined from Eq. (2) using the experimental values for v^*. We choose typical values for v^* and T/T_c of 100 m/s and 0.9 respectively, leading to $\tau_{in} \approx 2\times10^{-9}$ s and thus $B_T \approx 1.5$ T. As this is considerably larger than any of the fields for which the instability is observed in this study, the BS mechanism is not expected to be relevant.

It must be remembered, however, that if quasiparticle heating plays a role then the measured v^* values will be lower than the value in the absence of heating. Our estimate for B_T would thus be too large. We have therefore attempted an alternative analysis of our data in terms of the BS theory by comparing the experimental values of $P^*=I^*V^*$ with the theoretically predicted dependence on B/B_T. This does indeed result in fitted values of B_T somewhat lower than 1.5 T, but the agreement between experiment and theory was rather poor, implying that quasiparticle heating is not the dominant cause of the field dependence of v^*. We note also that pinning forces tended to cause this analysis to underestimate B_T. Finally, the reversibility of the transition at the instability point also provides strong evidence that we are in a field regime well below B_T. Overall, the role of quasiparticle heating in determining the instability behavior appears to be small in our samples.

Spatial inhomogeneity of the quasiparticle distribution has been shown to cause an increase in v^* at low fields.[5] Based on the above parameters we obtain the diffusion length of the quasiparticles $(D\tau_{in})^{1/2}=3\times10^{-7}$ m. Except very close to T_c this is greater than the vortex core size, but it becomes less than the intervortex spacing for fields below about 0.02 T. Although the critical velocity typically shows a decrease out to fields somewhat larger than 0.02 T, a small uncertainty in the diffusion length leads to a large uncertainty in the expected crossover field. Therefore, a nonuniform quasiparticle distribution may indeed be of importance at low fields.

We note also two other effects which may be significant. First, the vortices will tend to flow along regions with a

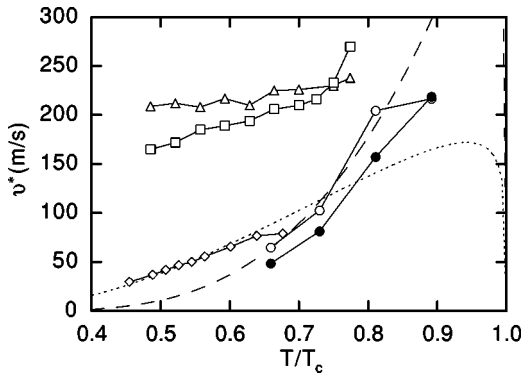

FIG. 6. Temperature dependence of the fitted critical vortex velocity for sample C at 0.7 T (◇), sample D at 0.3 T (○), and sample F at 0.2 T (△) and 0.8 T (□). The directly determined v^* values for sample D at 0.3 T (●) are also shown for comparison. The fitted curves are described in the text.

higher than average concentration of defects, especially at low fields where elastic interactions between the vortices are weak. The local inelastic scattering time may be less in these regions,[25] thus contributing to an increase in v^* at low fields. Secondly, if the vortex solid melts into a vortex liquid then any spatial nonuniformity in the quasiparticle distribution will be washed out by the random motion of the vortices. This is consistent with our previous findings[15] of a correlation between the melting transition in sample E and the disappearance of a strong field dependence in v^*. Melting of the vortex lattice could also significantly alter any thermal nonuniformity, an effect which is not included in the BS theory.

The critical vortex velocity determined from fits to Eq. 8 is plotted as a function of reduced temperature (T/T_c) in Fig. 6 for sample C at 0.7 T, sample D at 0.3 T, and sample F at 0.2 and 0.8 T. The values of v^* for sample D at 0.3 T determined from the I-V plot are also shown, to demonstrate again the similarity between the fitted and directly measured results.

For all of the samples v^* is an increasing function of temperature, implying that τ_{in} is the main contributor to the temperature dependence in Eq. (2). Electron-phonon scattering is expected to lead to the form $\tau_{in} \propto T^{-n}$ with $n=3$, but fits using this function lead to unphysical values for the exponent ($n \approx$ 6–10). We therefore provide fits based on electron-electron scattering, in which the scattering rate scales with the density of quasiparticles. The dotted and dashed lines in Fig. 6 show fits of Eq. (2) to the data from samples C and D, respectively, where we have used $\tau_{in} = A \exp[m\Delta(T)/k_B T]$ and $\Delta(T) = 1.76 k_B T_c (1 - T/T_c)^{1/2}$. We see excellent agreement with the data points using the parameters $A = 1.6 \times 10^{-10}$ s and $m=1$ for sample C, and $A = 1.4 \times 10^{-11}$ s and $m=2$ for sample D. A similar quality of fit was found for the other multilayer samples using the same functional form for τ_{in}. The different values found for m in samples C and D could be interpreted as indicating scattering mechanisms involving different numbers of electrons.[4,7] However it is difficult to say for certain that the differences are not simply due to uncertainties in the v^*, D or T_c values, or to the different magnetic fields. Nevertheless, the present results confirm the recent findings in a similar low-T_c system[7] (a-Mo_3Si thin films) that electron-electron scattering dominates the energy relaxation at low temperatures. In our case the dominance of electron-electron scattering over electron-phonon scattering is not surprising considering the reduced dimensionality associated with the multilayer structure of the films.

We note from Figs. 5 and 6 that the magnitude of v^* tends to increase as the superconducting layer thickness decreases, which is also consistent with increased electron-electron interactions in lower dimensions. The only exception to this rule comes from sample F, which Fig. 6 shows has a relatively temperature independent v^* that could not readily be fitted using the above expression for τ_{in}. The single layer in this film is considerably thicker than the individual superconducting layers in the other samples, implying that the dominant relaxation mechanism in sample F may instead be electron-phonon scattering. However, if this is the case it is surprising that sample F exhibits the highest critical vortex velocities of all the samples, indicating that it has the largest scattering rate.

V. DISCUSSION

The form we have chosen to represent pinning leads to several qualitative changes in the predicted I-V characteristics. For example, the measured instability current I^* becomes greater than in the absence of pinning, because higher currents are needed to force vortex motion at velocities near v^*. The field or temperature at which the backbending of the I-V curves is expected to give way to smooth transitions now corresponds to a value of α lower than 8. This crossover can be observed experimentally as long as the vortex motion is homogeneous throughout the sample. However, if the vortex solid melts into a vortex liquid, then just above the melting field plastic motion of rather large correlated vortex regions occurs.[1] Different parts of the sample may then undergo the LO instability at slightly different currents. This immediately leads to a broadening of the transition into a more stepwise increase, irrespective of the value of α. We see this behavior in samples D and E (see Figs. 3 and 4) where there is a well characterized melting of the vortex solid[15] which coincides with the change from sharp to stepwise transitions at the instability.

Our attempts at fitting the data have shown that neither the original LO I-V equation [Eq. (4)] nor the modified version [Eq. (8)] are able to fully capture the sharpness of the instability in fields below about 0.1 T. This is clearly apparent in the low field data of Fig. 4, where, although the resistance increases faster than linear near I^*, the I-V curves actually become flatter on the log-log plot right up until the sudden transition. There is very little extra increase in the resistivity associated with the onset of nonequilibrium effects. Similar behavior was observed in all of the other samples at low fields. By contrast, at higher fields, even when the transition itself is discontinuous, there are clear signs of an upturn in the I-V characteristics immediately preceding the instability (e.g., Figs. 2 and 3). To obtain reasonable fits in the low field regime the fitted curves must be allowed to extend beyond I^* before they start to bend backwards. This causes a slight exaggeration in the field depen-

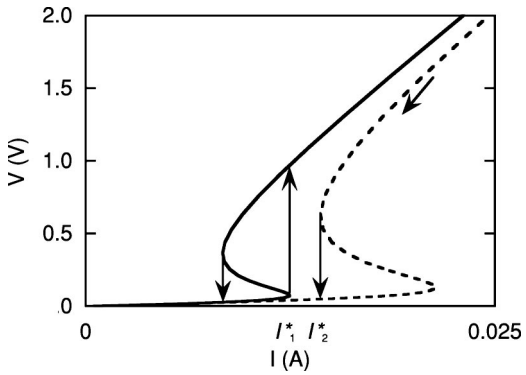

FIG. 7. Calculated I-V curves showing the difference between upward and downward current sweeps. The two curves are identical except for the value of V^* which is equal to 0.07 V on the left hand curve and 0.12 V on the right hand curve, corresponding to a slight decrease in τ_{in} on the downward current sweep.

dence of the fitted v^* values relative to the experimental transition points.

To explain the extreme sharpness of the transitions at low fields we note that τ_{in} is dominated by electron-electron scattering, and thus depends on the density of normal electrons available to scatter from inside the vortex core. As soon as the vortex velocity approaches v^* quasiparticles begin to escape from the vortex cores, thereby decreasing the number of electrons available to scatter from. The inelastic scattering time thus becomes an increasing function of the vortex velocity, and the critical velocity itself begins to decrease. The actual instability occurs slightly before the point predicted by the I-V equation assuming a constant τ_{in}, causing the observed dramatic sharpening of the transition at low fields. At high fields the diffusion length of the quasiparticles becomes larger than the intervortex spacing, and the quasiparticle distribution is uniform, so no significant changes in τ_{in} would be expected to occur. The high field data therefore match the theoretical I-V curves very well.

The lack of hysteresis in any of the measured I-V curves is central to our conclusion that the instabilities are related to a nonequilibrium quasiparticle distribution rather than thermal effects. However, both Eqs. (4) and (8) do in fact allow for some hysteresis between upward and downward current sweeps (see Fig. 7), as has been observed experimentally in one study.[14]

A possible explanation for the lack of hysteresis can be obtained if we assume that above the instability the inelastic scattering time becomes less than below the instability. Such a decrease has been suggested by Samoilov *et al.*[14] to explain a *clockwise* hysteresis in I-V data from an a-Mo_3Si film, where the change in τ_{in} was attributed to increased electron-electron scattering in the normal state above I^*. According to Eqs. (2) and (3), a lower τ_{in} implies a higher value of V^*. The I-V curves on upward and downward current sweeps would therefore be similar to the solid and dotted lines in Fig. 7, respectively. On an upward sweep the instability occurs at I_1^*, while on a downward sweep the transition back into the superconducting state would occur at I_2^* due to the decrease in τ_{in}. However, the downward transition is prevented from occurring at I_2^* because this would return τ_{in} and V^* to their low current values, and in this case the sample cannot support the superconducting state at any current above I_1^*. Thus the instability occurs at the same current on a downward or an upward current sweep, and the curve is reversible. The parameters used for the two curves in Fig. 7 are $\alpha=30$, $\beta=0$, and $V^*=0.07$ or 0.12 V for the upward and downward current sweeps respectively, demonstrating that only a relatively small change in V^* is needed for a significant movement of the I-V curve (this corresponds to only a factor of 3 change in τ_{in}).

VI. CONCLUSIONS

We have observed LO type instabilities in Ta/Ge-based multilayers and thin films with a wide range of pinning strengths. The complexity in the vortex phase diagram associated with the different regimes of pinning is reflected in the behavior of the instability. The inclusion in the I-V equation of a simple model of pinning forces has allowed us to capture many of the features of the experimental data. The temperature dependence of the critical vortex velocity extracted from the analysis implies that electron-electron scattering dominates the energy relaxation in these samples, consistent with results on similar systems. We have explained the lack of hysteresis in the I-V curves in terms of a decrease in the inelastic scattering time above the instability. A full theoretical investigation would clearly be of interest, treating simultaneously the dynamic pinning force and the non-equilibrium quasiparticle distribution. Nevertheless, our model and experimental observations highlight many of the features which a complete theory must exhibit.

ACKNOWLEDGMENTS

This work was supported by the New Zealand Public Good Science Fund and Marsden Fund, the Research Corporation Cottrell College Science Award (CC4444), and the New Zealand/USA Cooperative Science Program.

*Present address: Advanced Materials and Process Engineering Laboratory, Department of Physics and Astronomy, University of British Columbia, Vancouver, British Columbia V6T-1Z4, Canada.

[1] G. Blatter, M. V. Feigel'man, V. B. Geshkenbein, A. I. Larkin, and V. M. Vinokur, Rev. Mod. Phys. **66**, 1125 (1994).

[2] A. I. Larkin and Yu. N. Ovchinnikov, Zh. Éksp. Teor. Fiz. **68**, 1915 (1975) [Sov. Phys. JETP **41**, 960 (1976)].

[3] A. I. Larkin and Yu. N. Ovchinnikov, in *Nonequilibrium Superconductivity*, edited by D. N. Langenberg and A. I. Larkin (North-Holland, Amsterdam, 1986), p. 493.

[4] S. G. Doettinger, R. P. Huebener, R. Gerdemann, A. Kühle, S. Anders, T. G. Träuble, and J. C. Villégier, Phys. Rev. Lett. **73**, 1691 (1994).

[5] S. G. Doettinger, R. P. Huebener, and A. Kühle, Physica C **251**, 285 (1995).

[6] S. G. Doettinger, R. P. Huebener, S. Kittelberger, and C. C. Tsuei, Europhys. Lett. **33**, 641 (1996).

[7] S. G. Doettinger, S. Kittelberger, R. P. Huebener, and C. C. Tsuei, Phys. Rev. B **56**, 14 157 (1997).

[8] Z. L. Xiao and P. Ziemann, Phys. Rev. B **53**, 15 265 (1996).
[9] Z. L. Xiao, P. Voss-de Haan, G. Jakob, and H. Adrian, Phys. Rev. B **57**, 736 (1998).
[10] Z. L. Xiao, E. Y. Andrei, and P. Ziemann, Phys. Rev. B **58**, 11 185 (1998).
[11] Z. L. Xiao, P. Voss-de Haan, G. Jakob, Th. Kluge, P. Haibach, H. Adrian, and E. Y. Andrei, Phys. Rev. B **59**, 1481 (1999).
[12] L. E. Musienko, I. M. Dmitrenko, and V. G. Volotskaya, Pis'ma Zh. Éksp. Teor. Fiz. **31**, 603 (1980) [JETP Lett. **31**, 567 (1980)].
[13] W. Klein, R. P. Huebener, S. Gauss, and J. Parisi, J. Low Temp. Phys. **61**, 413 (1985).
[14] A. V. Samoilov, M. Konczykowski, N.-C. Yeh, S. Berry, and C. C. Tsuei, Phys. Rev. Lett. **7**, 4118 (1995).
[15] B. J. Ruck, J. C. Abele, H. J. Trodahl, S. A. Brown, and P. Lynam, Phys. Rev. Lett. **78**, 3378 (1997).
[16] A. I. Bezuglyj and V. A. Shklovskij, Physica C **202**, 234 (1992).
[17] H. L. Johnson, Ph.D. thesis, Victoria University of Wellington, 1993.
[18] H. L. Johnson and H. J. Trodahl, J. Phys.: Condens. Matter **7**, 1159 (1995).
[19] S. Ullah and A. T. Dorsey, Phys. Rev. Lett. **65**, 2066 (1990).
[20] S. Ullah and A. T. Dorsey, Phys. Rev. B **44**, 262 (1991).
[21] P. H. Kes and C. C. Tsuei, Phys. Rev. B **28**, 5126 (1983).
[22] Due to the collective nature of the pinning, for a large density of pinning sites the total pinning force may in fact vary as the square root of the area of the vortex. Therefore we have also tried using $F_p \propto [1+(V/V^*)^2]^{-1/2}$, but have found that this only leads to minor quantitative differences in the results of the fitting.
[23] At very low currents the vortex glass model actually predicts an exponential dependence of the voltage on the current, rather than a power law. However, this regime lies well below the voltage range where the instability is observed.
[24] W. J. Skocpol, in *Nonequilibrium Superconductivity, Phonons, and Kapitza Resistance*, edited by K. E. Gray (Plenum, New York, London, 1981), p. 559.
[25] For example, in areas with a high concentration of defects superconductivity will be suppressed leading to a greater than average density of normal electrons.